UC San Diego
UC San Diego Previously Published Works

Title

Nanosecond X-Ray Photon Correlation Spectroscopy on Magnetic Skyrmions

Permalink

Journal

ISSN

Authors

Seaberg, MH
Holladay, B
Lee, JCT
et al.

Publication Date

DOI

Peer reviewed

Nanosecond X-Ray Photon Correlation Spectroscopy on Magnetic Skyrmions

M. H. Seaberg,[1] B. Holladay,[2] J. C. T. Lee,[3,4] M. Sikorski,[1] A. H. Reid,[1] S. A. Montoya,[5,6] G. L. Dakovski,[1] J. D. Koralek,[1] G. Coslovich,[1] S. Moeller,[1] W. F. Schlotter,[1] R. Streubel,[7] S. D. Kevan,[3,4] P. Fischer,[7] E. E. Fullerton,[5,6] J. L. Turner,[1] F.-J. Decker,[1] S. K. Sinha,[2] S. Roy,[4,*] and J. J. Turner[1,†]

[1]*Linac Coherent Light Source, SLAC National Accelerator Laboratory, Menlo Park, California 94720, USA*
[2]*Department of Physics, University of California–San Diego, La Jolla, California 92093, USA*
[3]*Department of Physics, University of Oregon, Eugene, Oregon 97401, USA*
[4]*Advanced Light Source, Lawrence Berkeley National Laboratory, Berkeley, California 94720, USA*
[5]*Center for Memory and Recording Research, University of California–San Diego, La Jolla, California 92093, USA*
[6]*Department of Electrical and Computer Engineering, University of California–San Diego, La Jolla, California 92093, USA*
[7]*Materials Sciences Division, Lawrence Berkeley National Laboratory, Berkeley, California 94720, USA*
(Received 5 April 2017; published 9 August 2017)

We report an x-ray photon correlation spectroscopy method that exploits the recent development of the two-pulse mode at the Linac Coherent Light Source. By using coherent resonant x-ray magnetic scattering, we studied spontaneous fluctuations on nanosecond time scales in thin films of multilayered Fe/Gd that exhibit ordered stripe and Skyrmion lattice phases. The correlation time of the fluctuations was found to differ between the Skyrmion phase and near the stripe-Skyrmion boundary. This technique will enable a significant new area of research on the study of equilibrium fluctuations in condensed matter.

Ever since Einstein's paper on Brownian motion, fluctuations of matter in equilibrium has been a cornerstone in modern physics [1]. This provides the basis for phase transitions and critical phenomena in statistical mechanics [2], order parameter field theories in quantum criticality [3], the ergodic theory of conductance in metals [4], and understanding symmetry breaking in general, in solids [5]. From a theoretical standpoint, constructing the dynamic susceptibility $\chi(q, \omega)$ or a model Hamiltonian for a spin system can be, at the most fundamental level, akin to understanding the magnetic fluctuations. In the case of magnetic and strongly correlated electronic materials, the fluctuations of interest occur over a wide range of time and length scales, presenting a central challenge from both experimental and theoretical perspectives.

Spontaneous fluctuations at the nanoscale are known in many cases to have profound influence over material properties, such as transport, viscosity, or even determination of the system's thermodynamic phase. For example, spin fluctuations are considered to be an important component in stabilizing the topological magnetic structures called Skyrmions [6,7]. The Skyrmion phase originates from competition between the symmetric-type exchange $(S_i \cdot S_j)$ and antisymmetric-type Dzyaloshinskii-Moriya $(S_i \times S_j)$ interactions (see Fig. 1) [8,9]. Skyrmions have

been observed in a variety of chiral magnetic systems, that include MnSi [10], CoFeB [11], PtCoTa [12], FeCoSi [13], FeGe [14], IrCoPt [15], and multiferroic Cu_2OSeO_3 [16,17]. They have also been observed in many thin films with perpendicular anisotropy [18]. Experimental verification of Skyrmions in magnetic systems have come from small-angle neutron scattering, Lorentz TEM measurements, resonant x-ray scattering, and the topological Hall effect [19]. Apart from interesting physics, these topological entities can be moved coherently over macroscopic distances with very low currents and have the potential for use in advanced quantum computing and
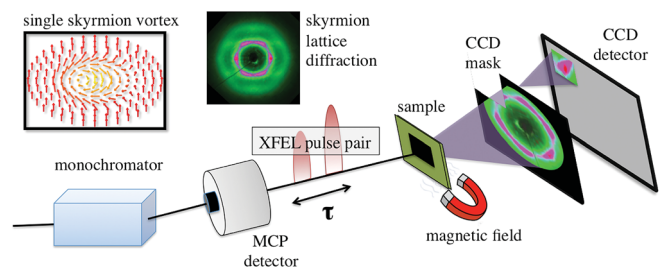

FIG. 1. Schematic depicting the geometry of the experiment at the LCLS [25], including the monochromator, the MCP detector which is used to sort the relative pulse height amplitude between pulse pairs, the pulse pair separated by time τ, the sample and applied magnetic field, the CCD mask to limit x-ray illumination on the CCD to a small region of interest, and the commercial (Andor) CCD. Inset: a cartoon of a single spin configuration of a chiral magnetic Skyrmion, a single unit of the Skyrmion lattice, and the resonant x-ray scattering from the Skyrmion hexagonal lattice, as measured at the ALS.

future memory devices. In spite of a large number of studies on Skyrmion textures and their related motion using electrical currents, very limited reports exist on the fluctuating nature of the order parameter [20,21]. In particular, there is no study of element specific measurements on fluctuations in a Skyrmion system, that which offers the information necessary to calculate the dynamic susceptibility $\chi(q, \omega)$ in a complex, multifunctional material from first principles [22].

To achieve a fundamental understanding of the fluctuations in a condensed phase, spatial and temporal correlations can be determined by the van Hove correlation function, $G(r, t)$, or measured via its space-momentum Fourier transform: the intermediate scattering function $S(q, t)$. One way to measure this is using x-ray photon correlation spectroscopy (XPCS) [23,24]. This is a coherent scattering method wherein random variations in the scattered intensity, or "speckle," are measured as a function of time. The speckle diffraction pattern is formed from interference of the scattered coherent beam due to sample heterogeneity. This relies on spatial coherence of the x rays and on a disorder length scale that is much greater than the x-ray wavelength.

The dynamics associated with spin heterogeneity are well known to occur in the nanosecond time range, according to the Landau-Lifshitz-Gilbert equation. This regime has so far been inaccessible to XPCS due to significant technical challenges, such as available coherent x-ray flux and detectors. Thus, in spite of their scientific importance, XPCS studies on time scales faster than 1 μs have not been possible. We note that the common pump-probe technique can access much shorter times for the study of excited states, but this is not suitable for studying spontaneous fluctuations since the system needs to be probed while in equilibrium.

In this Letter, we demonstrate that $S(q, t)$ can be measured on the nanosecond time scale using XPCS by directly probing the magnetic structure of the Skyrmion lattice (see Fig. 1) in a thin film of amorphous Fe/Gd, exhibiting a hexagonal lattice phase. This is 3 orders of magnitude faster then the current state-of-the-art measurements. The experiment was performed by using a pair of femtosecond x-ray pulses that are tuned to the Gd M_5 resonance ($\approx$1190 eV), sensitive to the magnetic moment of Gd. Magnetic diffraction peaks appear from the magnetic texture due to the Skyrmion lattice, providing experimental observation of first spontaneous magnetic fluctuations directly on the nanoscale. Near the stripe-Skyrmion phase boundary, we observe a more rapid fluctuation and a larger fraction of the magnetic structure exhibiting spatiotemporal fluctuations. In contrast, the magnetic vortex motion deeper in the Skyrmion phase is relatively slower. The method that we report here creates an opportunity to use femtosecond pulse pairs from an x-ray free electron laser (XFEL) [25] to study thermally induced, spontaneous nanoscale fluctuations in materials, an area of exploration that has not been possible until now.

In the conventional mode of XPCS, a series of speckle patterns is collected sequentially as a function of time from which the intensity-intensity autocorrelation $g_2(\tau)$ is calculated, related to $S(q, \tau)$, where τ is the time difference between successive pulses [26]. This has been used from the microsecond time scale to several hundreds of seconds [27–34]. For time scales below a microsecond, this method is impractical due to detector speed limitations, and available coherent x-ray flux. Alternatively, a two-pulse technique has been proposed that takes advantage of the high coherent flux and short pulse nature of XFELs [35]. This instead records the sum of two speckle patterns while adjusting τ between the pulse pair. The speckle contrast $C(q, \tau)$, which is related to $g_2(q, \tau)$, is calculated from this sum of the speckle patterns. This is the idea behind the use of a split-and-delay device, where XPCS can be conducted by splitting a single pulse from the XFEL into two equal pulses [36]. The split-and-delay device, however, has stringent requirements on the stability and alignment of the optics which makes its use nontrivial.

Here we use a two-bunch machine mode that produces two separate femtosecond pulses that are time delayed with respect to each other directly from the XFEL accelerator [37]. This mode uses two different Ti:sapphire laser systems to illuminate the linear accelerator cathode and creates two separate electron bunch sources. Each bunch is accelerated colinearly down the linac at 120 Hz, but in separate radio-frequency (rf) "buckets," allowing time delays in the nanosecond regime as bunches can be separated by integer multiples of the rf period, 350 ps.

The sample measured is a multilayer with 100 repetitions of alternating Fe (0.34 nm) and Gd (0.4 nm) layers grown by dc magnetron sputtering. This system can be adjusted in total thickness to optimize the scattering intensity and the alloy composition can be tuned so the Skyrmion phase occurs at room temperature [38]. They were deposited on 50 nm Si_3N_4 membranes and were measured in a forward scattering geometry. The samples were precharacterized at the coherent soft x-ray beam line (12.0.2.2) of the Advanced Light Source (ALS) [39] using a prescripted magnetic field cycle [40]. The sample was shown to exhibit an aligned stripe domain state and a Skyrmion state at room temperature between perpendicular magnetic fields of $\mu_0 H \approx 0-150$ and $\mu_0 H \approx 150-250$ mT, respectively (see Fig. 1 for an example).

Resonantly tuned coherent soft x-ray scattering was performed at the SXR beam line at the LCLS [41]. The pulse pair was set to the M_5 edge in Gd at 1190 eV using a 100 l/mm monochromator, with a bandwidth set by the exit slit to 1.0 eV [42,43]. The spot size on the sample was set to a diameter of 30 μm using a KB mirror system [44], and the detector (Andor Newton) was placed 1.4 m from the sample, such that the speckle size would be oversampled by the 13 μm pixel size of the detector.

We measured hexagonally symmetric resonant scattering from the Skyrmion lattice, with 100 nm vortex domains, in

the form of speckle diffraction. A 90×90 pixel region of interest (ROI) of the detector was centered on a magnetic Bragg peak at a diffraction angle of $2\theta = 0.3°$ (Fig. 1). The small ROI was used in order to acquire data at the repetition rate of the LCLS (120 Hz). An electromagnet was used to apply an out-of-plane magnetic field, with a tilt of $3.5°$ in order to reproduce a small, in-plane field [40]. A micro-channel plate (MCP) placed between the monochromator and the sample was used for monitoring the energies of each x-ray pulse individually. XFEL pulse pairs were selected under the condition that the pulse energies measured with the MCP were within 20% of each other [45].

To measure spontaneous fluctuations, the sample must be kept in equilibrium during the measurement. This requirement forces the intensity of the XFEL beam to be considerably reduced. At a repetition rate of 120 Hz, a sparse photon count was obtained on the detector which hindered the traditional techniques for extracting the contrast from the speckle pattern. The data must be analyzed using the methodology of quantum optics, such that the contrast can be calculated through photon statistics. We used a droplet algorithm to localize the photon positions and account for charge sharing between adjacent pixels, thus determining the number of photons in each speckle [46,47].

When measurements are made in the photon-counting regime, speckle contrast must be defined differently. In this case one must measure the probability distribution of detecting k photons in any given speckle:

$$P(k) = \frac{\Gamma(k+M)}{k!\Gamma(M)}\left(\frac{\bar{k}}{\bar{k}+M}\right)^k\left(\frac{M}{\bar{k}+M}\right)^M, \quad (1)$$

where $\Gamma(x)$ is the gamma function, M is the degrees of freedom in the speckle pattern, and $\bar{k}$ is the average number of photons [48]. M can then be extracted as a fit parameter for the measured distribution, and the speckle contrast can be calculated as $C = 1/\sqrt{M}$.

To compare the observations of the x-ray speckle patterns recorded on the detector to the probability distribution in Eq. (1), we calculate $P(k)$ by counting all the speckles with k photons in them and simply divide by the total number of speckles in the diffraction pattern. Figure 2 shows the probability $P(k)$ of detecting $k = 1$ to $k = 4$ photons per speckle, giving four unique ways to extract M per pair of XFEL shots fired. The data are plotted with $\bar{k}$, together with the error, all simulated contrast values for increasing shades of green between 0.2 and 1 in 20% increments, and the best fit to the data. Data for $P(k = 4)$, shown in Fig. 2(d), did not have good enough statistics for a reliable comparison. We also fit the ratio $\alpha(k) \equiv P(k)/P(k+1)$ for $k = 1$. This enforces self-consistency and gives another way to determine the contrast from the data.

XPCS measurements were performed in both the Skyrmion lattice phase at 210 and at 200 mT, closer to the stripe-Skyrmion boundary. In the Skyrmion phase, we
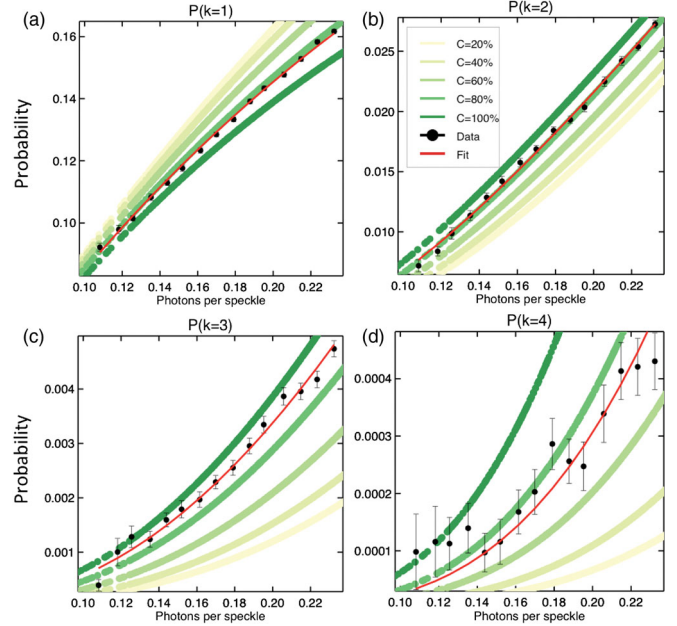

FIG. 2. Probability to scatter k photons, $P(k)$, for $k = 1-4$ photons at the Skyrmion peak measured through coherent soft x-ray resonant scattering in Fig. 2(a)–(d), respectively. The distributions are plotted with $\bar{k}$, the average photons per speckle. The black points are the binned data, the shades of green represent the range of contrast calculations for this range of data, and the red curve is the best fit of the data to Eq. (1).

use $\alpha(k)$ for $k = 1$ to extract the values of $C(q, \tau)$ as a function of time delay between pulses in Fig. 3, for $q = 0.06$ nm^{-1}. To confirm the results, we also analyze speckle patterns that contain speckles with exactly $k = 3$ photons and fit $P(k)$ using Eq. (1). We chose $k = 3$ in particular because of what we call "contrast dispersion." This is the measure of the spread in $P(k)$ as a function of contrast, allowing us to obtain a more precise value for $C(q, \tau)$ [compare Fig. 2(a) to Fig. 2(c)].

The final contrast curve generated from both $\alpha(k = 1)$ and the $P(k = 3)$ information was fit to the simplest model: a single exponential decay. Magnetic fluctuations related to the Skyrmion lattice ordering length scale are observed to exist on a ~4 ns time scale, an effect that has not been observed before (Fig. 3). We excluded the point at 0.7 ns from the exponential fit, which may be an indication of an oscillation in the correlation function as depicted qualitatively in Fig. 3. However, more data are required to verify this scenario. Although $C(q, \tau)$ seem to only drop by 10%, it should be noted that for two completely uncorrelated speckle patterns with equal intensity, the contrast is only reduced by a factor of $\sqrt{2}$ relative to that of a single pattern. From our observation of about 10% contrast reduction, we thus conclude that about one-third of the Skyrmion domain state fluctuates on a time scale of 4 ns, or faster.

We next investigate how the fluctuations change near the stripe-to-Skyrmion phase boundary, by lowering the
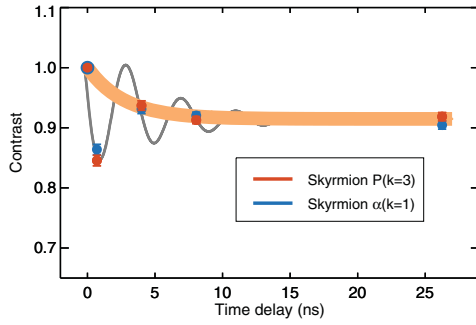
FIG. 3.   Contrast vs time delay in the Skyrmion phase at 210 mT. The blue data points are calculated based on a fit to $\alpha(1)$, the ratio between $P(1)$ and $P(2)$, using Eq. (1). A fit to $P(3)$ is shown for comparison (red data points). The orange curve represents a fit to an exponential, yielding a decay time of 4 ns. The (qualitative) oscillatory curve shown in gray is one possible solution for the apparent deviation from a simple exponential decay.

FIG. 4.   Contrast vs time delay near the Skyrmion-stripe phase transition at 200 mT. Blue data points are calculated based on a fit to $\alpha(1)$, the ratio between $P(1)$ and $P(2)$, using Eq. (1), with the fit for $P(3)$ shown for comparison (red data points). The blue curve represents a decay time consistent with the data, estimated at 300 ps.

applied magnetic field to 200 mT. We extract the contrast following the same procedure as for the Skyrmion phase mentioned above. In comparison to the Skyrmion lattice phase, the dynamics in this part of the phase diagram shown in Fig. 4 indicate that the system exhibits $80\% \pm 20\%$ domain fluctuations. In addition, the time constant drops considerably, from 4 ns to < 300 ps. This indicates larger, and more rapid fluctuations near the phase boundary.

The implicit assumption of equilibrium dynamics studies raises the question: Are the x rays promoting excitations in the system? Taking into account beam line optics, bandwidth, and the filtering, we estimate a maximum fluence of 0.15 mJ/cm^2 at the sample for this experiment. At this wavelength, this corresponds to a dose of $\approx 10^{-3}$ eV/atom. We calculate that this multilayered sample structure exhibits damage at a fluence of about 50 mJ/cm^2, or an energy dose of about 0.4 eV/atom [49]: well above our experimental conditions. To test the damage threshold experimentally, we systematically increased the fluence until we reached the point at which the scattered intensity became nonlinear with incoming pulse energy. This occurred at a fluence of 5 mJ/cm^2, indicating the threshold where sample modification can occur before damage sets in. Additionally, tracking the measured M values as a function of photon density did not reveal a noticeable deviation from Eq. (1), further confirming that the sample is not being modified with the first pulse.

The power of the method demonstrated here is not only an ability to measure the time scale of the magnetic fluctuations, but also that we can both associate this specifically with in-plane Skyrmion motion at the range of the Skyrmion-Skyrmion interaction, as well as with the fraction of fluctuating Skyrmion domains. Our data are consistent with other Skyrmion work such as GHz ferromagnetic resonance (FMR) modes observed in a similar Fe/Gd system [50], as well as with recent neutron spin echo spectroscopy experiments on fluctuating magnetic correlations in FeCoSi [51].
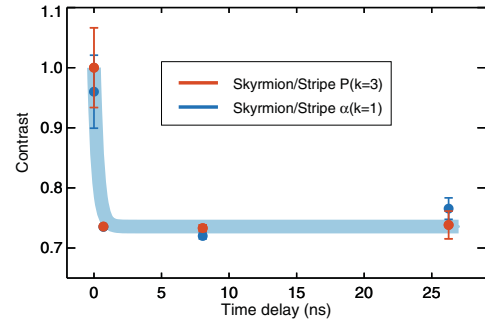
The quasiparticle equation of motion used for gyrotropic eigenmodes is most likely not applicable here since the rotational motion of these objects in the plane of the sample, perpendicular to the x-ray propagation vector, would not contribute to a decay in contrast of the speckle patterns [52]. It is clear that spin fluctuations, random motion, and lateral fluctuations of domain walls all contribute, and will be the focus for this method in the future, both from an experimental and a theoretical perspective.

The observation of nanosecond Skyrmion fluctuations through the use of x-ray pulse pairs, essentially using two XFELs simultaneously, is a technological breakthrough for the field of XPCS. This work demonstrates that through the use of developments in accelerator physics together with the speckle statistics formalism it is possible to perform nanosecond XPCS. A fundamental concept in solids is that of elementary excitations and how they relate to collective modes on different length scales, giving rise to the macroscopic properties of a material. The extension of XPCS into the nanosecond regime with this new XFEL advancement enables the study of a wide range of systems, including those that exhibit electronic and magnetic phenomena. These results indicate that XPCS can not only uncover a new regime of physical phenomena in the μeV range, but for even shorter times, may also be able to complement resonant inelastic x-ray scattering (RIXS) and inelastic neutron scattering in the future. Short bursts of soft x rays have many applications [53], but with the ability to separate pulses on these time scales, this technique will be a pivotal point for progress in new directions in condensed matter, especially those focused on the spin or orbital wave function of the electron.

———————

[*]sroy@lbl.gov
[†]joshuat@slac.stanford.edu

[1] A. Einstein, Ann. Phys. (Berlin) **322**, 549 (1905).
[2] H. E. Stanley, *Introduction to Phase Transitions and Critical Phenomena* (Oxford University Press, New York, 1971).
[3] S. Sachdev, *Quantum Phase Transitions* (Cambridge University Press, Cambridge, England, 2001).
[4] P. A. Lee, A. D. Stone, and H. Fukuyama, Phys. Rev. B **35**, 1039 (1987).
[5] J. Solyom, *Fundamentals of the Physics of Solids. Volume I, Structure and Dynamics* (Springer, Berlin, 2007).
[6] A. N. Bogdanov and U. K. Rößler, Phys. Rev. Lett. **87**, 037203 (2001).
[7] S. Mühlbauer, B. Binz, F. Jonietz, C. Pfleiderer, A. Rosch, A. Neubauer, R. Georgii, and P. Böni, Science **323**, 915 (2009).
[8] I. Dzyaloshinsky, J. Phys. Chem. Solids **4**, 241 (1958).
[9] T. Moriya, Phys. Rev. **120**, 91 (1960).
[10] F. Jonietz, S. Mühlbauer, C. Pfleiderer, A. Neubauer, W. Münzer, A. Bauer, T. Adams, R. Georgii, P. Böni, R. A. Duine *et al.*, Science **330**, 1648 (2010).
[11] W. Jiang, P. Upadhyaya, W. Zhang, G. Yu, M. B. Jungfleisch, F. Y. Fradin, J. E. Pearson, Y. Tserkovnyak, K. L. Wang, O. Heinonen *et al.*, Science **349**, 283 (2015).
[12] S. Woo, K. Litzius, B. Krüger, M.-y. Im, L. Caretta, K. Richter, M. Mann, A. Krone, R. Reeve, M. Weigand *et al.*, Nat. Mater. **15**, 501 (2016).
[13] W. Münzer, A. Neubauer, T. Adams, S. Mühlbauer, C. Franz, F. Jonietz, R. Georgii, P. Böni, B. Pedersen, M. Schmidt, A. Rosch, and C. Pfleiderer, Phys. Rev. B **81**, 041203 (2010).
[14] X. Z. Yu, N. Kanazawa, Y. Onose, K. Kimoto, W. Z. Zhang, S. Ishiwata, Y. Matsui, and Y. Tokura, Nat. Mater. **10**, 106 (2011).
[15] C. Moreau-Luchaire, C. Moutas, N. Reyren, J. Sampaio, C. A. F. Vaz, N. Van Horne, K. Bouzehouane, K. Garcia, C. Deranlot, P. Warnicke *et al.*, Nat. Nanotechnol. **11**, 444 (2016).
[16] S. Seki, X. Z. Yu, S. Ishiwata, and Y. Tokura, Science **336**, 198 (2012).
[17] Y. Onose, Y. Okamura, S. Seki, S. Ishiwata, and Y. Tokura, Phys. Rev. Lett. **109**, 037603 (2012).
[18] A. Fert, V. Cros, and J. Sampaio, Nat. Nanotechnol. **8**, 152 (2013).
[19] N. Nagaosa and Y. Tokura, Nat. Nanotechnol. **8**, 899 (2013).
[20] C. Pappas, E. Lelièvre-Berna, P. Falus, P. M. Bentley, E. Moskvin, S. Grigoriev, P. Fouquet, and B. Farago, Phys. Rev. Lett. **102**, 197202 (2009).
[21] C. Pappas, E. Lelièvre-Berna, P. Bentley, P. Falus, P. Fouquet, and B. Farago, Phys. Rev. B **83**, 224405 (2011).
[22] R. S. Markiewicz, I. G. Buda, P. Mistark, C. Lane, and A. Bansil, Sci. Rep. **7**, 44008 (2017).
[23] S. K. Sinha, Z. Jiang, and L. B. Lurio, Adv. Mater. **26**, 7764 (2014).
[24] M. Sutton, C.R. Phys. **9**, 657 (2008).
[25] C. Bostedt, S. Boutet, D. M. Fritz, Z. Huang, H. J. Lee, H. T. Lemke, A. Robert, W. F. Schlotter, J. J. Turner, and G. J. Williams, Rev. Mod. Phys. **88**, 015007 (2016).
[26] V. Degiorgio, Photon correlation techniques, in *Photon Correlation Spectroscopy and Velocimetry*, edited by H. Z. Cummins and E. R. Pike (Springer US, Boston, MA, 1977).
[27] F. Lehmkühler, P. Kwaśniewski, W. Roseker, B. Fischer, M. A. Schroer, K. Tono, T. Katayama, M. Sprung, M. Sikorski, S. Song *et al.*, Sci. Rep. **5**, 17193 (2015).
[28] J. Carnis, W. Cha, J. Wingert, J. Kang, Z. Jiang, S. Song *et al.*, Sci. Rep. **4**, 6017 (2014).
[29] S.-W. Chen, H. Guo, K. A. Seu, K. Dumesnil, S. Roy, and S. K. Sinha, Phys. Rev. Lett. **110**, 217201 (2013).
[30] K. A. Seu, S. Roy, J. J. Turner, S. Park, C. M. Falco, and S. D. Kevan, Phys. Rev. B **82**, 012404 (2010).
[31] J. J. Turner, K. J. Thomas, J. P. Hill, M. A. Pfeifer, K. Chesnel, Y. Tomioka, Y. Tokura, and S. D. Kevan, New J. Phys. **10**, 053023 (2008).
[32] O. G. Shpyrko, E. D. Isaacs, J. M. Logan, Y. Feng, G. Aeppli, R. Jaramillo, H. C. Kim, T. F. Rosenbaum, P. Zschack, M. Sprung, S. Narayanan, and A. R. Sandy, Nature (London) **447**, 68 (2007).
[33] C. Gutt, T. Ghaderi, V. Chamard, A. Madsen, T. Seydel, M. Tolan, M. Sprung, G. Grübel, and S. K. Sinha, Phys. Rev. Lett. **91**, 076104 (2003).
[34] A. C. Price, L. B. Sorensen, S. D. Kevan, J. Toner, A. Poniewierski, and R. Hołyst, Phys. Rev. Lett. **82**, 755 (1999).
[35] C. Gutt, L. M. Stadler, A. Duri, T. Autenrieth, O. Leupold, Y. Chushkin, and G. Grübel, Opt. Express **17**, 55 (2009).
[36] W. Roseker, S. Lee, M. Walther, H. Schulte-Schrepping, H. Franz, A. Gray, M. Sikorski, P. H. Fuoss, G. B. Stephenson, A. Robert *et al.*, in *Proceedings SPIE* (SPIE Digital Library, 2012), Vol. 8504, p. 85040I.
[37] F. Decker, S. Gilevich, Z. Huang, H. Loos, A. Marinelli, C. A. Stan, J. L. Turner, Z. V. Hoover, and S. Vetter, in *Proceedings of FEL2015* (2015), p. 634.
[38] S. A. Montoya, S. Couture, J. J. Chess, J. C. T. Lee, N. Kent, D. Henze, S. K. Sinha, M.-Y. Im, S. D. Kevan, P. Fischer *et al.*, Phys. Rev. B **95**, 024415 (2017).
[39] K. Chesnel, J. J. Turner, M. Pfeifer, and S. D. Kevan, Appl. Phys. A **92**, 431 (2008).
[40] J. C. T. Lee, J. J. Chess, S. A. Montoya, X. Shi, N. Tamura, S. K. Mishra, P. Fischer, B. J. McMorran, S. K. Sinha, E. E. Fullerton *et al.*, Appl. Phys. Lett. **109**, 022402 (2016).
[41] W. F. Schlotter, J. J. Turner, M. Rowen, P. Heimann, M. Holmes, O. Krupin, M. Messerschmidt, S. Moeller,

J. Krzywinski, R. Soufli *et al.*, Rev. Sci. Instrum. **83**, 043107 (2012).

[42] P. Heimann, O. Krupin, W. F. Schlotter, J. Turner, J. Krzywinski, F. Sorgenfrei, M. Messerschmidt, D. Bernstein, J. Chalupsky, V. Hajkova *et al.*, Rev. Sci. Instrum. **82**, 093104 (2011).

[43] K. Tiedtke, A. A. Sorokin, U. Jastrow, P. Juranic, S. Kreis, N. Gerken, M. Richter, U. Arp, Y. Feng, D. Nordlund *et al.*, Opt. Express **22**, 21214 (2014).

[44] J. Chalupsky, P. Bohacek, V. Hajkova, S. P. Hau-Riege, P. A. Heimann, L. Juha, J. Krzywinski, M. Messerschmidt, S. P. Moeller, B. Nagler *et al.*, Nucl. Instrum. Methods Phys. Res., Sect. A **631**, 130 (2011).

[45] Y. Sun, D. Zhu, S. Song, F.-J. Decker, M. Sutton, K. Ludwig, W. Roseker, G. Grübel, S. Hruszkewycz, G. B. Stephenson, P. H. Fuoss, and A. Robert, Proc. SPIE Int. Soc. Opt. Eng. **10237**, 102370N (2017).

[46] S. O. Hruszkewycz, M. Sutton, P. H. Fuoss, B. Adams, S. Rosenkranz, K. F. Ludwig, Jr., W. Roseker, D. Fritz, M. Cammarata, D. Zhu *et al.*, Phys. Rev. Lett. **109**, 185502 (2012).

[47] M. Sikorski, Y. Feng, S. Song, D. Zhu, G. Carini, S. Herrmann, K. Nishimura, P. Hart, and A. Robert, J. Synchrotron Radiat. **23**, 1171 (2016).

[48] J. Goodman, *Speckle Phenomena in Optics: Theory and Applications* (Roberts & Company, Greenwood Village, CO, 2007).

[49] J. Krzywinski (private communication).

[50] S. A. Montoya, S. Couture, J. J. Chess, J. C. T. Lee, N. Kent, M.-Y. Im, S. D. Kevan, P. Fischer, B. J. McMorran, S. Roy, V. Lomakin, and E. E. Fullerton, Phys. Rev. B **95**, 224405 (2017).

[51] L. J. Bannenberg, K. Kakurai, P. Falus, E. Lelièvre-Berna, R. Dalgliesh, C. D. Dewhurst, F. Qian, Y. Onose, Y. Endoh, Y. Tokura, and C. Pappas, Phys. Rev. B **95**, 144433 (2017).

[52] F. Büttner and M. Kläui, Magnetic Skyrmion dynamics, *Skyrmions* (CRC Press, Boca Raton, 2016), Chap. 8.

[53] G. L. Dakovski, P. Heimann, M. Holmes, O. Krupin, M. P. Minitti, A. Mitra, S. Moeller, M. Rowen, W. F. Schlotter, and J. J. Turner, J. Synchrotron Radiat. **22**, 498 (2015).